J. Geogr. Sci. 2011, 21(6): 1062-1076
DOI: 10.1007/s11442-011-0900-3

Composition, origin and weathering process of surface sediment in Kumtagh Desert, Northwest China

XU Zhiwei[1], *LU Huayu[1], ZHAO Cunfa[1], WANG Xianyan[1], SU Zhizhu[2], WANG Zhenting[3], LIU Hongyi[4], WANG Lixin[1], LU Qi[2]

1. School of Geographic and Oceanographic Sciences, the MOE Key Laboratory of Coast and Island Development, Nanjing University, Nanjing 210093, China;
2. Institute of Desertification Studies, Chinese Academy of Forestry, Beijing 100091, China;
3. College of Earth and Environmental Sciences, Lanzhou University, Lanzhou 730000, China;
4. Lanzhou Institute of Arid Meteorology, China Meteorological Administration, Lanzhou 730020, China

Abstract: Kumtagh Desert is one of the eight biggest deserts in China, but poorly investigated before our interdisciplinary study because of the difficulty of access. In this paper, 33 representative surface sediment samples were collected from the Kumtagh Desert and analyzed in the laboratory to obtain heavy mineral components and geochemical element contents. Results show that various kinds of heavy minerals are present in these samples, with high levels of epidote and hornblende. Si and Al take up a large part of chemical composition. Compared with the average composition of geochemical elements of the upper continental crust (UCC), except Si and Ca, all elements are depleted to a certain degree; Fe, Mg, Ca, P, Ti and Mn have high correlation coefficients in their contents. The mineral and geochemical composition of the Kumtagh Desert sediments have a similarity with that of rocks of Altyn Tagh Mountains, and the surface sediments of the alluvial/diluvial fans around the Altyn Tagh Mountains and that of the Taklamakan Desert, indicating that one major source of the Kumtagh Desert sediments is located in the Altyn Tagh Mountains. Alluvial deposits and lake sediments in Aqik valley and lower reaches of Shule River are prone to be eroded and transported by the strong northeasterly wind into the Kumtagh Desert, forming another source of the desert deposits. An A-CN-K ternary diagram shows that a weak degree chemical weathering by the loss of Na and K occurred in these sediments, whereas A-CNK-FM ternary diagram suggests that Fe and Mg have undergone a significant chemical differentiation. Physical weathering processes cause easy erosion and enrichment in fine particles for mafic minerals, thus coarse desert sand particles can be relatively depleted in Fe and Mg. The mineral and geochemical composition of sediments in arid regions experiencing less chemical weathering are mostly affected by physical weathering.

Keywords: minerals; geochemical elements; sediment provenance; weathering process; Kumtagh Desert

Received: 2011-04-21 **Accepted:** 2011-05-22

Foundation: The Global Change Program of China, No.2010CB950203; China National S&T Basic Work Program, No.2006FY110800; Natural Science Foundation of China, No.40930103, 41021002

Author: Xu Zhiwei (1988–), Ph.D Candidate, specialized in the physical geography.
E-mail: zhiweixu.nju@gmail.com; x-nju@163.com

***Corresponding author:** Lu Huayu (1968–), Ph.D and Professor, specialized in Quaternary environmental change and the physical geography. E-mail: huayulu@nju.edu.cn

1 Introduction

Recent studies on formation and evolution of deserts in northern China and its relationship with climate change have made considerable progresses. However, because of the difficulty of access, the Kumtagh Desert is the last of the eight biggest deserts in China to be systematically and scientifically investigated (E *et al*., 2006). In recent years, some researchers have focused on the geological background of the desert region (Zheng *et al*., 2000; Ritts and Biffi, 2000; Sun and Liu, 2006; Sun *et al*., 2009; Lu *et al*., 2010; Zhang and Sun, 2011) and its landscape features (Xia, 1987; Wang, 1987; Qu *et al*., 2005; E *et al*., 2008), as well as the morphological interpretations of dune landforms (Qu *et al*., 2007; Dong *et al*., 2008; E *et al*., 2008) and grain-size distribution of the sediments (He *et al*., 2009). However, the information about the sediment composition is very limited. Moreover, the origin of the desert deposits and weathering process during transportation have not been well documented.

Mineralogical and geochemical characteristics of desert deposits are widely used to trace sediment provenance (Weltje and Eynatten, 2004; Chen *et al*., 2007; Stevens *et al*., 2010) and sedimentary process (Nesbitt and Young, 1996; Nesbitt and Markovics, 1997; Muhs, 2004), as well as to reconstruct paleoclimatic changes (Nesbitt and Young, 1982; Ding *et al*., 2001; Chen *et al*., 2001; Újvári *et al*., 2008). Many studies have focused on sediment composition and provenance of the deserts in north China, e.g. Taklamakan Desert (Qian *et al*., 1993; Yang *et al*., 2007), the desert of Jungger Basin (Qian *et al*., 2001) and other dune fields (Xie and Ding, 2007; Stevens *et al*., 2010), while others use geochemical isotopic analyses to evaluate their contributions to the global dust production (Chen *et al*., 1995, 2007; Jickells *et al*., 2005; Zhang *et al*., 2005). However, these works did not include the weathering of desert sands during formation, transportation and deposition, and its influence on mineralogical and geochemical composition was also not considered.

The main factors that control mineralogical and chemical composition of silicate rocks are (1) source composition, (2) climate through chemical weathering, and (3) abrasion and sorting during the sediment transportation (Blatt *et al*., 1980; Johnsson *et al*., 1988; Johnsson *et al*., 1991; Nesbitt and Young, 1996; Young and Nesbitt, 1998; Ohta and Arai, 2007). Previous studies of sedimentary petrogenesis focused mainly on mineral chemical weathering and element migration related to *in-situ* weathering profiles (e.g. Nesbitt and Markovics, 1997; Chen *et al*., 1997; Ohta and Arai, 2007; Li *et al*., 2007). Nevertheless, effects of physical weathering on mineral or bulk chemical composition of sediment are given less attention (Nesbitt and Young, 1996), especially in arid regions where abrasion and sorting during transportation is considerable. In this study, 33 surface sediment samples were collected from Kumtagh Desert during the desert exploration in September 2007 and then analyzed in the laboratory with the following objectives: (1) to describe the mineralogical and geochemical characteristics of desert deposits in the Kumtagh Desert; (2) to investigate the source region of these sediments; (3) to evaluate the effect of physical weathering process on the mineralogical and geochemical composition of the desert sands.

2 Study area

The Kumtagh Desert is situated in the eastern part of the Tarim Basin, northwest to the Lop Nur Depression and south to the Altyn Tagh Mountains (89°57′–94°54′E, 39°07′–41°00′N)

(Figure 1). On the north of the desert locates Aqik Valley adjoining to the Kezile Tagh Mountain and to the east is the extensive Shule River flood plain. The Kumtagh Desert is the sixth biggest desert in China with an area of 2.28×10^4 km^2 (E *et al*., 2006). Various types of aeolian dunes cover the SW-NE inclined alluvial/diluvial plain of the northern Altyn Tagh Mountains, which is influenced by tectonic movement (Xia, 1987; E *et al*., 2006, 2008), and the unique pseudo-feathery dunes are distributed at the north central part of the desert (Qu *et al*., 2007; Dong *et al*., 2008). The annual precipitation of the desert region is less than 10 mm and therefore it is an extremely arid climate (E *et al*., 2006). NE, NNE and ENE winds combine to be the dominant group of winds, accounting for 45% of the winds, and the other group includes ESE and E winds, accounting for 23% (Dong *et al*., 2008). Seasonal rivers originating from the Altyn Tagh Mountains flow mainly northwards through the desert and cut several deep river gullies. At northwestern part of the Lop Nur Depression and lower reaches of the Shule River flood plain, the second largest Yardang landform in China is found (E *et al*., 2006; 2008).

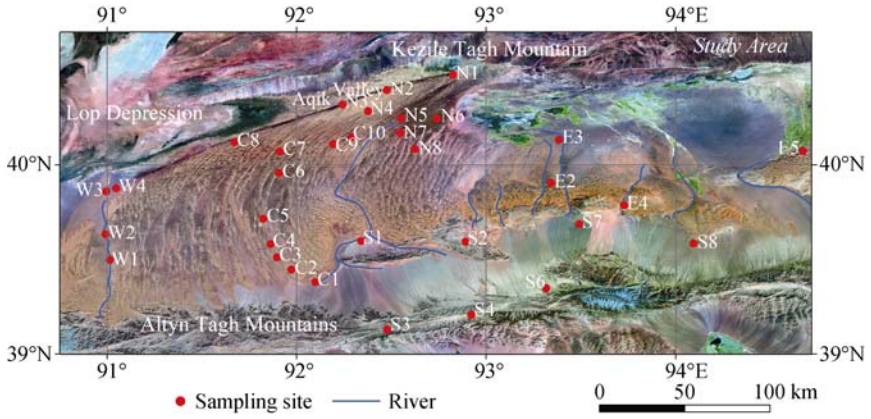

Figure 1 Geocover image of the Kumtagh Desert (from USGS). Solid red dots show locations of our sampling sites. Solid blue lines represent modern river patterns

3 Composition of the surface sediment

The 33 unconsolidated surface samples are divided into five subareas according to geographic location: the north (N region, n = 8), the west (W region, n = 4), the central (C region, n = 10), the south (S region, n = 7) and the east (E region, n = 4). S1, S2, S7 and S8 are dune sands or fluvial deposits from alluvial/diluvial fans of the northern Altyn Tagh Mountains; S3, S4 and S6 are fluvial sediments of the intermontane basin; sample E5 locates in Mingsha Hill; most of the other samples are aeolian sands. S3, S4, S6 and S8 all have fine grain-size distributions with high silt content, while others are course dune sands with a dominant component of medium to fine grade sand (He *et al*., 2009).

3.1 Mineralogical composition

The fine grain size fraction (<0.25 mm) of 25 samples was dry sieved to obtain heavy minerals using elutriation method. The ferromagnetic and electromagnetic fractions were extracted by a hand magnet or electromagnetic separator, and then weighed to calculate mass

faction. Heavy mineral grains of the three parts (ferromagnetic, electromagnetic and non-ferromagnetic fractions) were then counted under an optical microscope based on crystal feature, optical characteristic and chemical property to calculate the relative abundance of each mineral. The results show that more than 30 kinds of heavy minerals are present (Table 1), but with a low total proportion compared to the bulk sample. Generally, medium stable minerals (including epidote, zoisite and orthite) and stable minerals (including magnetite, hematite and goethite) have a high average content of 39.1% and 25.5% respectively, and content of very stable minerals (including tourmaline, zircon and rutile) is relatively low with a variation ranging from 0.6% to 7.95%. Samples from S and E regions have a considerable content of unstable minerals (mainly amphibole, average 28.5% in S region) while samples from N region have a relatively low content of 12.0% on average. Other minerals, such as garnet which ranges from 0.7% to 21.4%, anatas, leucoxene, barite and kyanite are present in almost all the samples, albeit with a rather low content. Pyrite was detected in some samples (frequency of samples with pyrite appearance is 56%); diopside was detected in S region (33%), C region (60%), W region (50%) and N region (12.5%); sillimanite was detected in C region (40%), W region (25%) and N region (12.5%); glaucophane was detected in S region (16.7%), W region (25%) and N region (12.5%); andalusite was present in sample W1 and N4; staurolite was present in sample S3 and S4; brookite was present in S3 and monazite was present in C10.

A Piper triangular diagram is used to show differences in mineral composition between samples (Qian *et al*., 2001). Six assemblages of heavy minerals are arrayed according to

Table 1 Regional average of the heavy minerals in Kumtagh Desert (%)

Sample	Total HM	Carbonate	Unstable minerals				Medium stable minerals				
			Amp	Px	Mica	Sum	Ep	Chl	Ap	Ttn	Sum
S (n=6)	1.45	4.4	28.5	0.4	0.1	29.0	31.5	0.7	0.5	0.4	33.1
C (n=5)	1.74	5.9	21.5	0.3	0.1	21.8	39.8	0.8	0.2	0.2	41.1
W (n=4)	1.52	7.0	22.8	0.3	0.1	23.3	45.9	0.4	0.2	0.2	46.8
N (n=8)	0.87	3.9	12.0	0.3	0.1	12.4	46.4	1.1	0.2	0.2	47.9
E4	1.80	3.9	49.7	0.8	0.9	51.4	14.3	0.8	0.4	0.8	16.4
E5	0.92	4.1	26.0	8.3	0.8	35.1	20.0	0.8	0.2	0.7	21.7
Total (n=25)	1.33	4.9	21.6	0.7	0.2	22.5	39.1	0.8	0.3	0.3	40.5

Sample	Stable minerals							Very stable minerals				
	Mgt	Hem & Gt	Grt	Ant	Leu	Brt	Ky	Sum	Tur	Zm	Rt	Sum
S (n=6)	13.0	13.3	3.3	M	M	M	m	29.7	0.2	3.2	0.3	3.7
C (n=5)	11.6	14.3	3.4	M	M	m	m	29.4	0.5	1.2	0.2	1.9
W (n=4)	9.7	8.9	2.7	M	m	M	m	21.4	0.3	1.1	0.1	1.5
N (n=8)	14.1	16.4	2.9	M	m	0.3	M	33.7	0.3	1.6	0.2	2.1
E4	7.1	10.1	9.3	M	m	M	m	26.5	0.2	1.4	0.2	1.8
E5	9.7	5.7	21.4	M	M	M	0.0	36.8	0.2	1.8	0.3	2.2
Total (n=25)	12.2	13.3	4.1	M	M	0.1	M	29.8	0.3	1.8	0.2	2.3

Amp-amphibole, Ant-anatas, Ap-apatite, Bry-barite, Chl-Chlorite, Ep-epidote, Grt-garnet, Gt-goethite, Hem-hematite, Leu-Leucoxene, Px-Pyroxene, Ky-kyanite, Mgt-magnetite, Rt-rutile, Ttn-titanite Tur-tourmaline, Zm-zircon; Carbonate includes calcite and dolomite; Hm-heavy minerals, M-small amount, m-present.

their physical and chemical stability (a. Amp+Px, b. Ep, c. Chl+Mica, d. Ttn+Ap, e. Hem+Gt+Mgt, f. Grt+Tur+Ant+Rt+Zm+Leu) and then plotted on a ternary diagram (Figure 2). Point congregations of the samples show that S region has significant a high Amp+Px content, while N region has a relatively high content of Ep and opaque iron minerals. Mineral assemblages of C and W regions show a high content of amphibole and epidote similar to S region. E5 in Mingsha Hill has a high garnet and pyroxene concentration inconsistent with main body of the desert. Generally, only slight differences exist among mineral assemblages of different regions in the Kumtagh Desert, indicating a relatively simple origin of the desert sands.

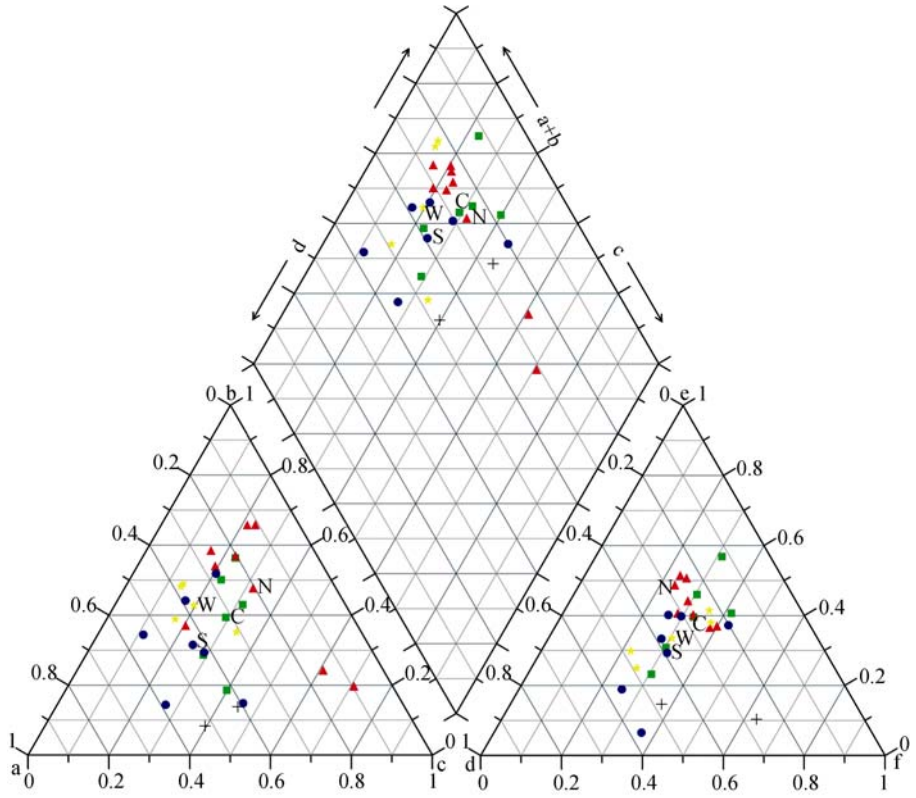

Figure 2 Mineral assemblage of surface sediments in Kumtagh Desert. a. Amp+Px; b. Ep; c. Chl+Mica; d. Ttn+Ap; e. Hem+Gt+Mgt+Ilm (ilmenite); f. Grt+Tur+Ant+Rt+Zm+Leu. Heavy dots show the samples: blue dot-S region, green dot-C region, yellow dot-C region, red dot-N region, cross point-E region.

3.2 Bulk geochemical composition

33 surface samples of the Kumtagh Desert were measured for major element abundance using X-ray fluorescence spectrometry (XRF) in the Center of Modern Analysis, Nanjing University. About 5 g of the samples were ground in an agate mill to <63 μm. Loss on ignition (LOI) was obtained by weighing after 10 h of calcination at 960℃. Some 0.6 g of each sample was mixed with dilithium tetraborate ($Li_2B_4O_7$:$LiBO_2$ = 67:33) flux (flux:sample = 11:1) in a Pt-Au crucible, fusing with LiBr (40 mg ml^{-1},0.6 ml) in a muffle oven to make fusion sample disc, and thereafter measured by a ARL9800XP+XRF Spectrometer. Concen-

trations of major elements were analyzed by comparing with standard samples and control experiments. Analytical uncertainties are 0.5% for SiO_2 and 0.2% for Al_2O_3. The relative error of CaO, K_2O, Fe_2O_3 and TiO_2 is less than 5% and less than 10% for MgO, Na_2O, P_2O_5 and MnO. The elemental concentrations are expressed as weight of oxide (%) with all iron expressed as Fe_2O_3.

Major elemental concentrations are presented in Table 2. On average, these samples have high Si (71.68±0.10%) and Al (10.16±0.11%). Compared with the average composition of the upper continental crust (UCC), these samples are depleted in Al, Ti, Fe, Mn, Mg, Na, K and P, but slightly enriched in Si and Ca. UCC-normalized major element distributions of these surface sediments show a similarity to that of the Taklamakan Desert (Table 2 and Figure 3g, Qian *et al*., 1993; Yang *et al*., 2007), but with a relatively low concentration of CaO. Compared to the average composition of loess and dust, these samples are poorer in Ti, Fe, Mn and Mg, but significantly enriched in CaO contents in comparison to the loess. The lower CaO in loess may indicate an intensive Ca mobilization during chemical weathering after dust deposition (Chen *et al*., 1997, 2001). When compared to PAAS, typical products of continental chemical weathering (Taylor and McLennan, 1985), the desert deposits are significantly higher in Ca and Na, but depleted in Al, Fe, Mn, Fe and P. Variances exist between different regions: samples of the S region, primary materials eroded from the Altyn Tagh Mountains, are enriched in Ti, Fe, Mg, Mn and Ca relative to the UCC, which means

Table 2 Average of the major elements in Kumtagh Desert (%) and comparison with other aeolian deposits

Sample		SiO_2	TiO_2	Al_2O_3	Fe_2O_3[i]	MnO	MgO	CaO	Na_2O	K_2O	P_2O_5
S (n=7)		60.67	0.59	10.50	4.18	0.07	3.23	7.93	2.03	2.18	0.13
E (n=4)		70.47	0.33	9.80	2.73	0.06	2.10	5.43	2.64	1.73	0.07
C (n=10)		74.11	0.33	10.46	2.44	0.05	1.22	3.22	2.90	2.49	0.07
W (n=4)		74.61	0.33	10.59	2.30	0.05	1.32	3.00	2.89	2.43	0.06
N (n=8)		77.41	0.33	9.45	2.10	0.04	0.98	2.58	2.55	2.26	0.06
Kumtagh (n=33)	Mean	71.68	0.38	10.16	2.75	0.05	1.71	4.31	2.59	2.27	0.08
	St. D	0.10	0.34	0.11	0.34	0.28	0.54	0.52	0.16	0.17	0.36
Loess(n=12)[a]		66.40	0.73	14.20	4.81	0.07	2.29	1.02	1.66	3.01	0.15
Paleosol (n=13)[b]		65.18	0.75	14.79	5.12	0.08	2.21	0.83	1.41	3.15	0.11
Red clay (n=5)[c]		63.75	0.76	15.05	5.28	0.08	2.89	0.90	1.16	3.00	0.15
Taklamakan1 (n=24)[d]		62.05	0.46	10.60	3.10	0.06	2.20	7.88	2.58	2.11	0.10
Taklamakan2 (n=42)[e]		73.25	0.39	10.18	2.36	0.06	1.58	7.30	2.33	2.40	0.16
Dust (n=4)[f]		55.58	0.74	13.20	5.50	0.10	2.94	4.68	1.45	2.54	0.21
UCC[g]		66	0.5	15.2	5	0.06	2.2	4.2	3.9	3.4	0.5
PAAS[h]		62.8	1.0	18.9	7.22	0.11	2.2	1.3	1.2	3.7	0.16

[a] Average of 12 loess samples from Chinese Loess Plateau (Chen *et al*., 2001). [b] Average of 13 paleosol samples from Chinese Loess Plateau (Chen *et al*., 2001). [c] Average of 5 red clay samples from Chinese Loess Plateau (Chen *et al*., 2001). [d] Average of 24 sand samples from Taklamakan Desert (Yang *et al*., 2007). [e] Average of 42 sand samples from Taklamakan Desert (Qian *et al*., 1993). [f] Average of 4 dust samples, data from four published articles of Lanzhou, 1993 (Shi *et al*., 1995), Harbin, 2002 (Xie *et al*., 2006), Beijing, 2006 (Zhang *et al*., 2008) and Nanjing, 2006 (Li *et al*., 2009). [g] The Upper Continental Crust (UCC; Taylor and McLennan, 1985). [h] The post-Archean Australian average shale (PAAS; Taylor and McLennan, 1985). [i] Total iron expressed as Fe_2O_3.

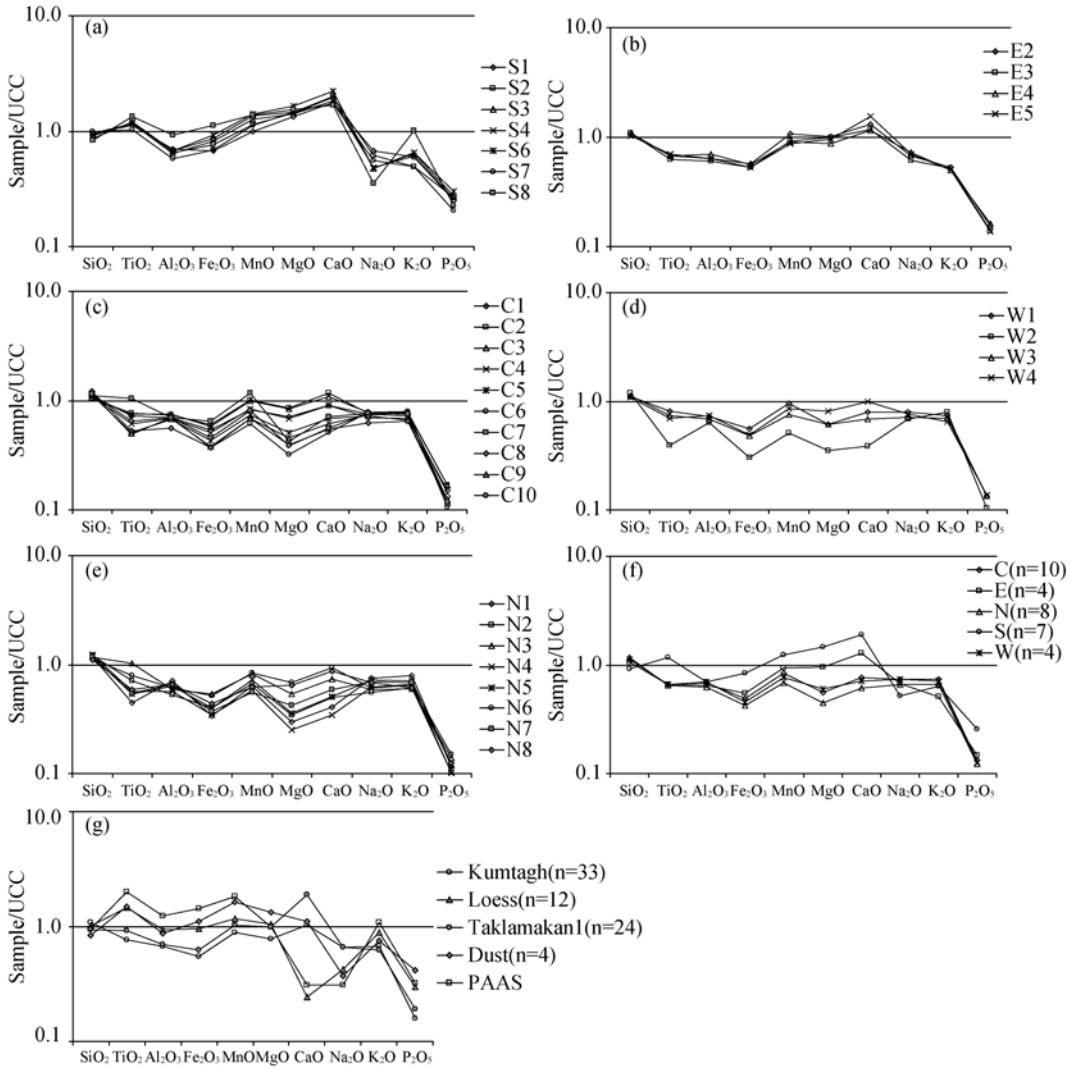

Figure 3 UCC-normalized major element patterns. a-S region; b-E region; c-C region; d-W region; e-N region; f-mean value of each region; g-mean value of Kuntagh Desert, mean value of Taklamakan Desert (Taklamakan1 (n = 24); Table 2), the average loess (Loess (n = 12); Table 2), the average dust (Dust (n = 4), Table 2) and comparison with the standard PAAS; The UCC and PAAS values were used from Taylor and McLennan (1985).

the original deposits from glacier or fluvial erosion have undergone less chemical weathering. Compared to the S region, samples of the E region have a slight paucity of Ti, Fe, Mg and Ca contents, but element distribution is still consistent. Samples from the W region and C region are further depleted in Ti, Fe, Mg, Ca, K and P along with increasing distance away from their main source region, the Altyn Tagh Mountains. As a result, samples from the N region, which are the most far north, have almost all major elements concentration lower than the UCC except for Si. The coefficients of variability (CV) of K, Na, Al and Si are relatively low while Fe, Mg, Ca, P, Ti and Mn show high values of CV and standard deviation (Figure 4 and Table 2). In addition, Fe, Mg, Ca, P, Ti and Mn have strong positive correlation with each other and high negative correlation with Si, suggesting that Fe, Mg, Ti, Mn

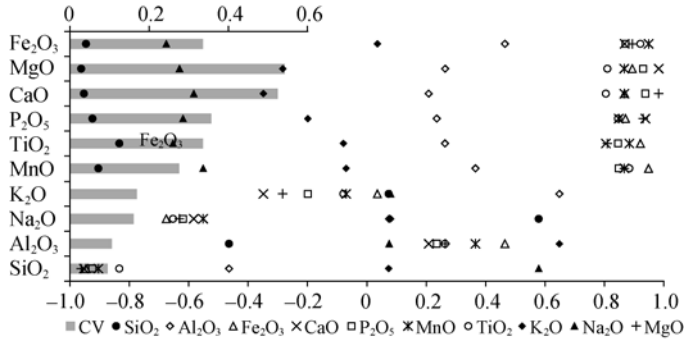

Figure 4 Correlation coefficients between major elements (bottom axis) and coefficient of each variance (CV, top axis)

and Ca may display similar geochemical behavior or element mobility during weathering and deposition.

4 Discussion

4.1 Provenance of the sediment in the Kumtagh Desert

The great dunes are developed overlying the alluvial/diluvial plain in the north piedmont of the Altyn Tagh Mountains (E *et al*., 2006, 2008). Seasonal rivers originating from the Altyn Tagh Mountains flow northwards through the hinterland of the desert and leave several deep gullies, where thick fluvial/lacustrine formations underlying the dunes were exposed for easy erosion. Traces of palaeo-drainage system (e.g. gravel relief) were found in the northern part of the desert (E *et al*., 2006), indicating long distance transportation of eroded materials from the Altyn Tagh Mountains into the hinterland of the desert by the rivers. Therefore the origin of the surface sediments in the Kumtagh Desert could have a close relationship with surrounding mountains. Mineralogical analysis suggests the desert sand has a dominant amphibole content, while the appearance of metamorphic minerals (e.g. diopside, glaucophane, sillimanite, staurolite), high Si, Ca, Na content and low Al, K, Na, P content are consistent with the sand composition of the Taklamakan Desert, which is of typical character for metamorphic and volcanic rock sources. The bedrock of the north Altyn Tagh Mountains consists of predominant Proterozoic or Archean gneisses, schist, phyllite and granite, the same as the rock type of extensively-outcropping schist and gneisses appearing in the Kunlun Mountain and the Tianshan Mountain (Qian *et al*., 1993; Yang *et al*., 2007), while the rock type of Kezile Tagh Mountain in the north is mostly Carboniferous carbonate and clastic rocks. As such it could be concluded that the major Altyn Tagh Mountains are sand sources of the Kumtagh Desert: products of mountain erosion were transported into the basin by fluvial system from the Altyn Tagh Mountains, and then blown and sorted by wind to form aeolian sand dunes. Erosional remnant landscapes (e.g. gravel relief, gullies, Yardang, gravel and sand ground) and aeolian dunes are alternately distributed, giving the Kumtagh Desert a general fragmented appearance. Large volumes of material from underlying fluvial/lacustrine deposits could be easily deflated by wind to form the dune landforms in place. In addition, wide-ranging Yardangs are distributed at northwestern Lop Nur Depression and

the lower reaches of Shule River extended flood plain (E *et al*., 2006). Those alluvial/lacustrine deposits at Aqik Valley and the lower reaches of Shule River are prone to be eroded by strong northeastern wind and transported into the desert, which contributes another source for the desert deposits.

4.2 Weathering process of desert sand in the Kumtagh Desert

4.2.1 A-CN-K diagram

A-CN-K ternary diagrams based on the mass-balance principle, feldspar leaching experiments and thermodynamic calculation of mineral stability are widely used to predict the trend of continental chemical weathering and alteration of mineralogical or geochemical components (Nesbitt and Young, 1982; Chen *et al*., 2001; Li *et al*., 2007). The trendline from the UCC to PAAS represents a typical early stage of continental chemical weathering. Data points of samples from the Kumtagh Desert concentrate around the UCC (Figure 5), indicating that chemical compositions of these samples are similar to the UCC and have undergone hardly any or weak chemical weathering with a slight leaching of Na and Ca, and further evidenced by low CIA (Chemical Index of Alteration) values mostly below 50. In general, the A-CN-K ternary diagram reveals that surface sediments of the Kumtagh Desert are exposed to a lack of effective chemical weathering under the extremely arid climate.

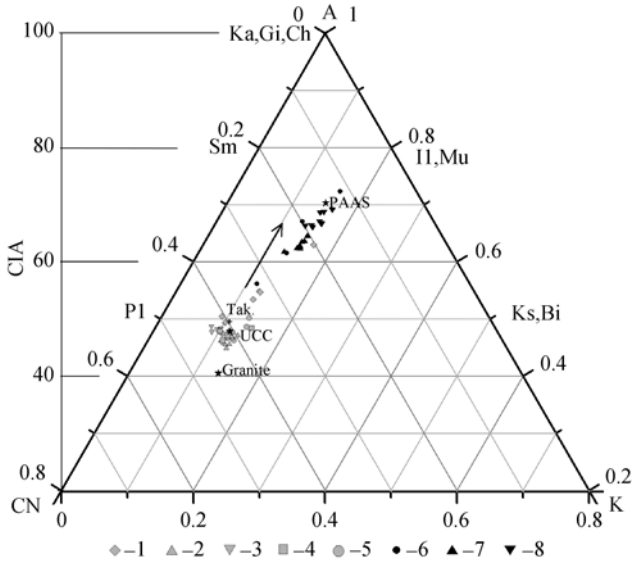

Figure 5 A-CN-K ternary diagram of the Kumtagh Desert. A=Al_2O_3, C=CaO, N=Na_2O, K=K_2O, CaO is the amount of CaO associated with the silicate fraction of the bulk sample, details of the calculations are provided by Nesbitt and Young (1982). 1-S region, 2-C region, 3-E region, 4-W region, 5-N region, 6-dust (Table 2), 7-loess (Table 2), 8-paleosol (Table 2). The standard PAAS and UCC values were used from Taylor and McLennan (1985). Granite-Granite rocks with high calcium (Turekian and Wedepohl, 1961). Tak.-the average composition of Taklamakan Desert (Taklamakan1 (n=24); Table 2). Bi-biotite, Ch-chlorite, Gi-gibbsite, Il-illite, Ka-kaolinite, Ks-K-feldspar, Mu-muscovite, Pl-plagioclase, Sm-smectite.

4.2.2 A-CNK-FM diagram

A-CN-K diagrams are used to predict chemical weathering intensity and variation of min-

eralogical or geochemical components through alkalis and Al content but fails to reflect migration or weathering of other elements. The coefficients of variability (CV) in Fe, Mg and Ti are relatively high and these elements show a strong positive correlation, indicating that Fe and Mg have gone through significant differential weathering or migration processes. The A-CNK-FM pattern is used to show variations in Fe and Mg abundances (Figure 6, Nesbitt and Young, 1996): Total Fe and Mg contents (FM value) of the desert deposits vary significantly and show a decreasing trend from the S region to N region, while Al and other alkalis have slightly increases. Considering the chemical composition of biotite (Bi, $K_{0.9}[Mg+Fe]_3Ti_{0.05}Al_{1.1}Si_{2.9}O_{10}[OH]_2$) and hornblende (Hb, $Na_1Ca_2[Mg+Fe]_5Al_1Si_7O_{22}[OH]_2$), most samples plot within the Feldspar (Fs) – Biotite (Bi) – Hornblende (Hb) compositional triangle (Figure 6, triangle defined by the dashed lines), indicating that chemical compositions of these deposits are mainly controlled by these minerals. To better understand chemical differentiation in Fe and Mg abundances, Quartz (Qz, SiO_2), K-feldspar (Ks, $KAlSi_3O_8$), Albite (Ab, $NaAlSi_3O_8$), Anorthite (An, $CaAl_2Si_2O_8$), Biotite (Bi) and Hornblende (Hb), these six rock-forming minerals are chosen to calculate the proportions of minerals in all sediments based on the A-CNK-FM diagram and XRD diffraction diagram of some samples (Figure 7, e.g. sample S1). Table 3 shows the transform matrix for mesonormative mineral calculation and the results presented in Table 4 indicate that the calculated average proportion of total femic minerals decreases from the S region to N regions accompanied with the increasing felsic mineral content. The estimated plagioclase content remains largely unchanged. The estimated proportion of K-feldspar is low in the S and E region, mostly because the potassium was preferentially partitioned into biotite, which had a relatively high calculated proportion due to the high Fe and Mg contents of the samples. Indeed the content of K-feldspar is expected to be constant, since it has more stability than albite or anorthite under

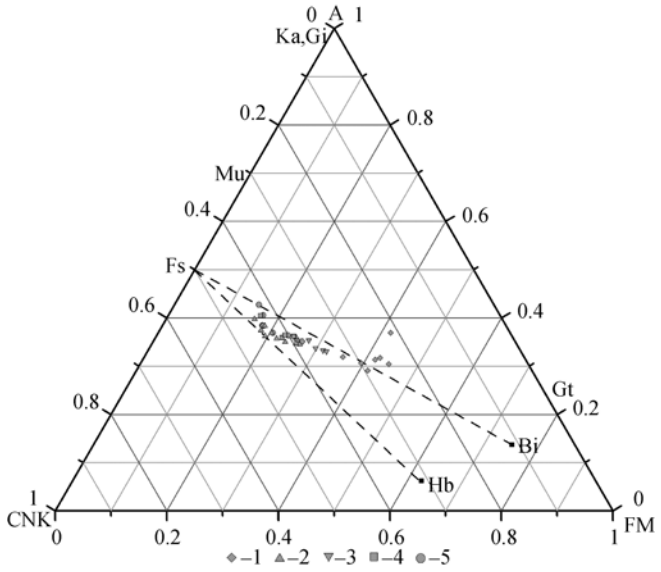

Figure 6 A-CNK-FM ternary diagram of the Kumtagh Desert. A = Al_2O_3, C = CaO, N = Na_2O, K = K_2O, F = FeOt, Mg = MgO, CaO is the amount of CaO associated with the silicate fraction of the bulk sample. 1-S region, 2-C region, 3-E region, 4-W region and 5-N region. The standard PAAS and UCC values were taken from Taylor and McLennan (1985). Bi-biotite, Fs-feldspar, Gi-gibbsite, Gt-garnet, Hb-hornblende, Ka-kaolinite, Mu- muscovite.

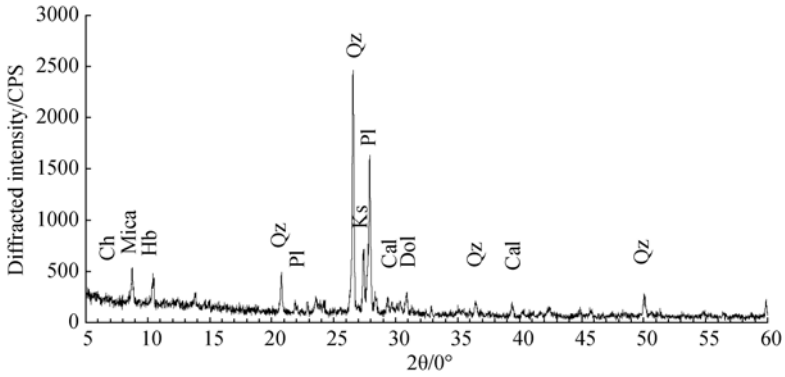

Figure 7 XRD diffraction diagram of the Kumtagh Desert (Sample S1). Ch-chlorite, Hb-hornblende, Qz-quartz, Pl-plagioclase, Ks-K-feldspar, Cal-calcite, Dol-dolomite.

Table 3 Transform matrix for mesonormative mineral calculation

Ab	An	Ks	Bi	Hb	Qz	Transform matrix
3	2	3	2.9	7	1	SiO_2
0.5	1	0.5	0.55	0.5	0	Al_2O_3
0	0	0	3	5	0	FeOt + MgO
0.5	0	0	0	0.5	0	Na_2O
0	1	0	0	2	0	CaO*
0	0	0.5	0.45	0	0	K_2O

Table 4 Results of mesonormative mineral calculation in the Kumtagh Desert (weight %)

Sample	Ab	An	Ks	Bi	Hb	Qz	Pl	Fs	Felsic	Femic
S (n=7)	18.3	11.7	0.6	30.3	1.1	36.0	30.0	30.6	66.6	31.4
E (n=4)	21.0	9.2	5.0	12.2	5.3	43.2	30.2	35.1	79.2	17.5
C (n=10)	22.4	8.0	12.9	4.2	8.8	42.3	30.4	43.3	85.6	13.0
W (n=4)	22.8	8.5	11.8	6.0	6.8	43.3	31.2	43.1	86.3	12.8
N (n=8)	20.3	7.4	11.1	5.3	5.3	49.5	27.7	38.8	88.3	10.6
Kumtagh(n=33)	20.9	8.8	8.8	11.2	5.6	43.0	29.7	38.5	81.5	16.8

Ab-albite, An-anorthite, Ks-K-feldspar, Bi-biotite, Hb-hornblende, Qz-quartz, Pl-plagioclase, Fs-total feldspar, Felsic-total felsic minerals, Femic-total femic minerals.

thermodyamic and kinetic considerations. Femic minerals such as biotite and hornblende have prefect cleavage, less physical and chemical stability, and the lamellar crystal form of biotite, easily abraded and weathered during transportation and then sorted, resulting in preferential enrichment in the fine-grained sediments.

The surface sediments of the Kumtagh Desert show high variations in Fe, Mg and Ti but low in Na and K. The A-CN-K diagram indicates that these deposits undergo a low degree of chemical weathering by loss of Na and Ca, and the A-CNK-FM diagram reveals significant chemical differentiations in Fe and Mg contents (Trend1 in Figure 8), but little changes in Na, K and Al. Mineral proportions were calculated using a matrix algebra approach and the results show that femic minerals (e.g. biotite and hornblende) rich in Fe and Mg are prone to

mechanical abrasion and preferential comminution during transportation. This yields the destruction of femic minerals in the coarse sand, resulting in the dearth of Fe and Mg in the coarse-grained sediment (Nesbitt and Young, 1996). If mass-balance was considered, comminution and sorting of femic minerals cause distinct chemical differentiation of Fe and Mg: fine-grained femic minerals would accumulate in the silt or clay component of the sediments and be mechanically separated from coarse-grained component by hydraulic or aeolian sorting during transportation, leading to enrichment of Fe and Mg in fine-grained component and depletion in the coarse residue. Compared with the chemical composition of typical aeolian deposits, loess and dust of East Asia, the weathering trend of samples from the Kumtagh Desert (Trend 1, Figure 8) is divergent from the trend exhibited by the fine aeolian deposits (Trend 2, Figure 8), which shows a significant increase in Al proportion (Here Trend 2 may be more right inclined, even parallel to the A-CNK axis line, however, this cannot be determined without secure composition of primary material). Fine-grained aeolian deposits are more enriched in Fe, Mg and Ti than the coarse desert sands (Figure 3g and 8). Assuming that the sediments of the S region represent the original composition of eroded material from high mountains, the divergent lines of Trend 1 and Trend 2 would be caused by mechanical abrasion and sorting during transportation: preferential abrasion and comminution of femic minerals are sorted and enriched in fine-grained sediment, and then mechanically separated from the coarse residue by the following hydraulic/aeolian sorting (aeolian sorting especially) and subsequently transported away from the desert area, leading to the relative deficit of Fe and Mg in the coarse desert sand.

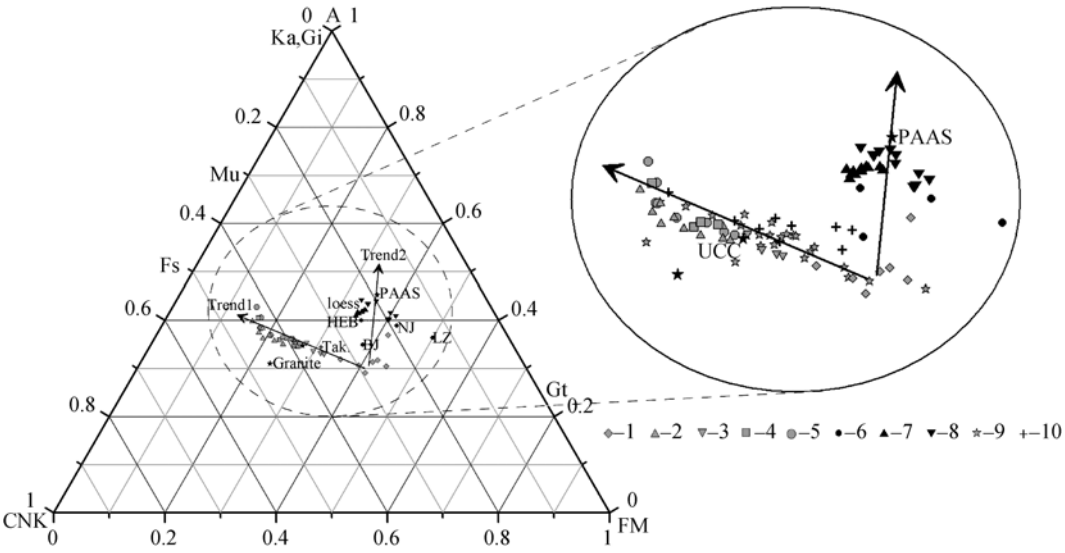

Figure 8 A-CNK-FM ternary diagram of the Kumtagh Desert, Taklamakan Desert, loess, dust and weathering trends. 1-S region, 2-C region, 3-E region, 4-W region, 5-N region, 6- dust (Table 2), 7-loess (Table 2), 8-paleosol (Table 2), 9-aeolian sand deposits of the Taklamakan Desert (Taklamakan1, Table 2), 10-the Taklamakan Desert (Taklamakan2, Table 2).

4.3 Chemical differentiation and elemental migration during deposition in the arid region

The main factors controlling mineralogical and geochemical composition of siliciclastic de-

posits are the source, climate during chemical weathering, and abrasion and sorting during transportation (Blatt *et al*., 1980; Johnsson *et al*., 1988; Johnsson *et al*., 1991; Nesbitt and Young, 1996; Young and Nesbitt, 1998; Ohta and Arai, 2007). Detailed work about the effects of abrasion and sorting on bulk composition in the absence of chemical weathering has been done by Nesbitt and Young (1996). An example in a glacio-fluvial system reveals that primary mafic minerals of the bedrock are preferentially concentrated in mud, subjected to abrasion and subsequent sorting. In arid regions, clastic deposits eroded from the high mountains are mainly controlled by glaciations and freeze-thaw processes, and then transported into the basin by subsequent hydraulic process or mass movement. Because of the extreme arid climate, sediments from Kumtagh are subject to very little or no significant chemical weathering. Thus, mechanical abrasion and sorting during transportation impart significant influences on bulk composition and mineralogy in the arid regions. Mechanical comminution includes abrasion occurring primarily within the glacier environment (Nesbitt and Young, 1996) and later abrasion by particles colliding, as well as possible dissolution or conversion of minerals, which makes it easy for mafic minerals to be eroded and enriched in the fine fraction. The fine-grained sediment would later be separated by subsequent differential sorting during hydraulic and aeolian transportation (aeolian sorting especially), generating fine aeolian deposits with higher abundances of Fe and Mg in the form of downwind dust deposition. That is different from the *in-situ* weathering profile, where usually elements would be leached by solution or minerals would be converted due to chemical weathering, and insoluble elements such as Fe, Al and Ti would not be mechanically transported or deposited allochthonously but enriched in the *in-situ* weathering profile. Figure 8 shows the two chemical differentiation trends (Trend 1 and Trend 2) experienced by surface sediments from the Kumtagh Desert, the Taklamakan Desert, loess and dust. Physical weathering processes (mechanical abrasion and sorting) account for this kind of chemical differentiation in the arid regions.

5 Conclusions

Detailed mineralogical and geochemical studies have been conducted in order to obtain heavy mineral components and geochemical element contents of surface sediments collected from the Kumtagh Desert. The results indicate one major source of the desert sand is located in the Altyn Tagh Mountains. Statistical analysis reveals that Fe, Mg, Ca, P, Ti and Mn have high correlation coefficients in their contents and an A-CNK-FM ternary diagram suggests that Fe and Mg have suffered significant chemical differentiation, though an A-CN-K ternary diagram suggests a weak degree of chemical weathering by loss of Na and K occurring in these desert deposits. Physical weathering processes (abrasion and sorting) preferentially erode mafic minerals and enrich them in the resultant fine particle fraction. Thus coarse desert sand particles are relatively depleted in Fe and Mg. The mineral and geochemical composition of sediments in arid regions with low levels of chemical weathering are therefore mostly affected by physical weathering processes.

Acknowledgment

We are grateful to Dr. Thomas Stevens, Royal Holloway, University of London for revising

this paper. We thank Mrs. Jia Youzhen and Mr. Zhang Mengqun for their laboratory assistance, and Ms. Wang Haini for her help in English writing.

References

Blatt H, Middleton G, Murray R, 1980. Origin of Sedimentary Rocks. Prentice-Hall, Inc.

Chen G Y, Dai X R, Zhang M J, 1995. Study on the heavy minerals in the dustfall of the severe duststorm numbered 930505 in Lanzhou area, Gansu Province. *Journal of Desert Research*, 15(4): 374–377. (in Chinese)

Chen J, An Z S, Liu L W *et al*., 2001. Variations in chemical compositions of the eolian dust in Chinese Loess Plateau over the past 2.5Ma and chemical weathering in the Asian inland. *Science in China* (*Series D*), 31(2): 136–145.

Chen J, Ji J F, Chou G *et al*., 1997. Geochemistry of the chemical weathering intensity of the loess profile in Luochuan, Shaanxi Province. *Science in China* (*Series D*), 27(6):531–536.

Chen J, Li G J, Yang J D *et al*., 2007. Nd and Sr isotopic characteristics of Chinese deserts: Implications for the provenances of Asian dust. *Geochimica et Cosmochimica Acta*, 71(15): 3904–3914.

Chen Y, Chen J, Liu L W, 2001. Chemical composition and characterization of chemical weathering of late Tertiary red clay in Xifeng, Gansu Province. *Journal of Geomechanics*, 7(2): 167–175. (in Chinese)

Ding Z L, Sun J M, Yang S L *et al*., 2001. Geochemistry of the Pliocene red clay formation in the Chinese Loess Plateau and implications for its origin, source provenance and paleoclimate change. *Geochimica et Cosmochimica Acta*, 65(6): 901–913.

Dong Z B, Qu J J, Wang X M *et al*., 2008. Pseudo-feathery dunes in the Kumtagh Desert. *Geomorphology*, 100(3/4): 328–334.

E Y H, Su Z Z, Wang J H *et al*., 2006. Outcome and scientific significance of integrated investigation in Kumtag Desert. *Journal of Desert Research*, 26(5): 693–697. (in Chinese)

E Y H, Wang J H, Yan P *et al*., 2008. Evolution of palaeo-drainage system and its relationship with the formation of desert landform in the Kumtag Desert. *Acta Geographica Sinica*, 63(7): 725–734. (in Chinese)

He Q, Yang X H, Huo W *et al*., 2009. Characteristics of sand granularity from Kumtag Desert and its environmental significance. *Journal of Desert Research*, 29(1): 18–22. (in Chinese)

Jickells T D, An Z S, Andersen K K *et al*., 2005. Global iron connections between desert dust, ocean biogeochemistry, and climate. *Science*, 308: 67–71.

Johnsson M J, Stallard R F, Lundberg N, 1991. Controls on the composition of fluvial sands from a tropical weathering environment: Sands of the Orinoco River drainage basin, Venezuela and Colombia. *Geological Society of America Bulletin*, 103(12): 1622–1647.

Johnsson M J, Stallard R F, Meade R H, 1988. First-cycle quartz arenites in the Orinoco River Basin, Venezuela and Colombia. *Journal of Geology*, 96: 263–277.

Li X S, Han Z Y, Chen Y Y *et al*., 2009. Characteristics and source of rain dust in Nanjing on March 11, 2006. *Quaternary Sciences*, 29(1): 43–54. (in Chinese)

Li X S, Han Z Y, Yang S Y *et al*., 2007. Chemical weathering intensity and element migration features of the Xiashu Loess profile in Zhenjiang. *Acta Geographica Sinica*, 62(11): 1174–1184. (in Chinese)

Lu H Y, Wang X Y, Li L P, 2010. Aeolian sediment evidence that global cooling has driven late Cenozoic stepwise aridification in central Asia. In: Clift P D, Tada R, Zheng H (eds.). Monsoon Evolution and Tectonics–Climate Linkage in Asia. *Geological Society, London, Special Publications*, 342: 29–44.

Muhs D, 2004. Mineralogical maturity in dunefields of North America, Africa and Australia. *Geomorphology*, 59(1–4): 247–269.

Nesbitt H, Markovics G, 1997. Weathering of granodioritic crust, long-term storage of elements in weathering profiles, and petrogenesis of siliciclastic sediments. *Geochimica et Cosmochimica Acta*, 61(8): 1653–1670.

Nesbitt H, Young G, 1996. Petrogenesis of sediments in the absence of chemical weathering: effects of abrasion and sorting on bulk composition and mineralogy. *Sedimentology*, 43(2): 341–358.

Nesbitt H W, Young G M, 1982. Early Proterozoic climates and plate motions inferred from major element chemistry of lutites. *Nature*, 299(21): 715–717.

Ohta T, Arai H, 2007. Statistical empirical index of chemical weathering in igneous rocks: A new tool for evaluating the degree of weathering. *Chemical Geology*, 240(3/4): 280–297.

Qian Y B, Wu Z N, Ishii T *et al*., 1993. The constituent characteristics of sand materials and sand sources of Taklamakan Desert. *Journal of Desert Research*, 13(4): 32–38. (in Chinese)

Qian Y B, Zhou X J, Li C S *et al*., 2001. Multi-sources of sand minerals for the deserts in the Jungger Basin. *Journal of Desert Research*, 21(2): 182–187. (in Chinese)

Qu J J, Liao K T, Zu R P *et al*., 2007. Study on formation mechanism of feather-shaped sand ridge in Kumtag Desert. *Journal of Desert Research*, 27(3): 349–354. (in Chinese)

Qu J J, Zuo G C, Zhang K C *et al*., 2005. Relationship between the formation and evolution of the Kumtag Desert and the regional Neotectonic movement. *Arid Land Geography*, 28(4): 424–428. (in Chinese)

Ritts B D, Biffi U, 2000. Magnitude of post-Middle Jurassic displacement on the central Altyn Tagh fault system, Northwest China. *Geological Society of American Bulletin*, 112(1): 61–74.

Shi Y X, Dai X R, Li J T *et al*., 1995. On the wind-blown deposits from a heavy dust fall numbered "930505" in Lanzhou, North-Central China. *Acta Sedimentologica Sinica*, 13(3): 76–82. (in Chinese)

Stevens T, Palk C, Carter A *et al*., 2010. Assessing the provenance of loess and desert sediments in northern China using U-Pb dating and morphology of detrital zircons. *Geological Society of America Bulletin*, 122: 1331–1344.

Sun J M, Li Y, Zhang Z Q *et al*., 2009. Magnetostratigraphic data on the Neogene growth folding in the foreland basin of the southern Tianshan Mountains. *Geology,* 37, 1051–1054.

Sun J M, Liu T S, 2006. The age of the Taklimakan Desert. *Science*, 312: 1621.

Taylor S R, McLennan S M, 1985. The Continental Crust: Its Composition and Evolution. London: Blackwell, 277.

Turekian K K, Wedepohl K H, 1961. Distribution of the elements in major units of the earth crust. *Bulletin of the Geological Society of America*, 72(2): 175–192.

Újvári G, Varga A, Balogh-Brunstad Z, 2008. Origin, weathering, and geochemical composition of loess in southwestern Hungary. *Quaternary Research*, 69(3): 421–437.

Wang S J, 1987. Formation of Aqik valley in the east of Lop Nor. Lop Nor Comprehensive Scientific Expedition Team, Xinjiang Branch of Chinese Academy of Sciences, Lop Nor Scientific Expedition and Research. Beijing: Science Press, 60–67. (in Chinese)

Weltje G J, von Eynatten H, 2004. Quantitative provenance analysis of sediments: Review and outlook. *Sedimentary Geology*, 171(1–4): 1–11.

Xia X C, 1987. Basic character of Kumtag Desert. Lop Nor Comprehensive Scientific Expedition Team, Xinjiang Branch of Chinese Academy of Sciences, Lop Nor Scientific Expedition and Research. Beijing: Science Press, 52–59, 78–94. (in Chinese)

Xie J, Ding Z L, 2007. Compositions of heavy minerals in Northeastern China sandlands and provenance analysis. *Science in China* (*Series D*), 50(11): 1715–1723.

Xie Y Y, He K, Zhou J *et al*., 2006. Chemical characteristic of dust storm deposits in Harbin and its matter origin. *Geographical Research*, 25(2): 255–261. (in Chinese)

Yang X B, Zhu B Q, White P D, 2007. Provenance of aeolian sediment in the Taklamakan Desert of western China, inferred from REE and major-elemental data. *Quaternary International*, 175(1): 71–85.

Young G, Nesbitt H, 1998. Processes controlling the distribution of Ti and Al in weathering profiles, siliciclastic sediments and sedimentary rocks. *Journal of Sedimentary Research*, 68(3): 448–455.

Zhang S, Liu P, Jin C S *et al*., 2008. Geochemistry of the heavy dust fall on 17 April 2006 in Beijing. *Marine Geology & Quaternary Geology*, 28(3): 36–42. (in Chinese)

Zhang X Y, Wang Y Q, Wang D *et al*. Characterization and sources of regional-scale transported carbonaceous and dust aerosols from different pathways in coastal and sandy land areas of China. *Journal of Geophysical Research*, 2005, 110(D15): D15301.

Zhang Z Q, Sun J M, 2011. Palynological evidence for Neogene environmental change in the foreland basin of the southern Tianshan range, northwestern China. *Global and Planetary Change*, 75, 56–66.

Zheng H, Powell C, An Z *et al*., 2000. Pliocene uplift of the northern Tibetan Plateau. *Geology*, 28(8): 715–718.